

PHOTONIC CRYSTALS

https://doi.org/10.1070/QEL16783

Peculiarities of electromagnetic field distribution in a finite one-dimensional photonic crystal at oblique incidence of radiation

V.V. Kapaev, M.N. Zhuravlev

Abstract. **The effect of increasing an electric field E is investigated for oblique incidence of radiation on a finite one-dimensional photonic crystal. The peculiarities in the field distribution in the structure $E(x)$ are found to be due to the interference of counterpropagating Bloch waves; therefore, the conditions for increasing the field to a maximum value $|E|_{max}$ coincide with those for achieving the maximum band gap E_g of an infinite crystal. It is shown that a significant (several times for structures with 30 periods) growth of $|E|_{max}$ is observed with increasing angle of incidence θ for wavelengths λ, which correspond to transmission maxima T nearest to the band gap boundaries. The increased interference of the counterpropagating Bloch modes is caused by an enhancement of the x-component contrast (perpendicular to the planes of the layers) of the wave numbers k_{1x}/k_{2x} in the structure layers. Along with this, there also arise characteristic features in the distribution of $E(x)$ associated with the vanishing of the forbidden band width. In this case, the field distribution in all periods is the same. Two types of such features are observed in the case of oblique incidence. The former takes place for p-polarisation at an angle of incidence θ, which is an analogue of the Brewster angle. The latter corresponds to the situation when the length of each structure layer is equal to an integer of half-waves. This occurs simultaneously for s- and p-polarisations and is observed in a limited range of layer widths only for the second and highest forbidden bands.**

Keywords: *photonic crystal, forbidden band, angle of incidence, radiation polarisation.*

1. Introduction

Electromagnetic field distribution in finite layered periodic structures (one-dimensional photonic crystals) has a number of features (an increase in the field amplitude [1], an increase in the density of states and a decrease in the group velocity [2]) at parameter values corresponding to the boundaries of the forbidden bands of an infinite crystal. These features are due to the interference of counterpropagating Bloch waves (Floquet modes) and manifest themselves at wavelengths λ corresponding to the maxima of the dependences of transmission T on λ. This was first noticed in [1], where it was shown that in a layered periodic structure formed in a disturbed surface layer of CdS subjected to annealing during the first laser pulse, the field intensity can dramatically increase under irradiation by subsequent pulses, which leads to an increase in the efficiency of annealing. The most prominent effects can occur in nonlinear media. Scalora et al. [3] demonstrated the possibility of increasing the second harmonic generation intensity by two to three orders of magnitude for the GaAs/AlAs structure containing 20 periods in comparison with a homogeneous medium of the same length. Similar phenomena are observed when light propagates in a waveguide grating with a finite number of elements [4]. This system in the first approximation can also be described as a one-dimensional photonic crystal. Hopman et al. [4] present a technique for studying the field distribution in such systems based on the measurement of the scattered light and point to the wide possibilities of practical use of the effect.

Gorelik and Kapaev [5] analysed the peculiarities of the field distribution in a finite periodic structure with normal incidence of radiation and showed the correlation of the maximum field value $|E|_{max}$ with the band gap of an infinite periodic structure. In this paper, we will generalise the results for the case of oblique incidence. For definiteness, as in [5], the objects are opal matrices, i.e. artificial opals constructed from close-packed silicon oxide globules (balls) [6–8], and mesoporous photonic crystal films. The latter are obtained by anodic etching of doped silicon or aluminium [9, 10]. As a result, films are formed whose layers are characterised by different degrees of porosity and retain the periodicity of the corresponding one-dimensional crystal lattice.

The most significant increase in the field amplitude in the structure is observed when the values of the parameters correspond to the first maxima of the dependences of the transmission coefficient T on the radiation frequency $T(\nu)$ [or on the wavelength $T(\lambda)$] located to the right and left of the boundaries of the forbidden bands. For a sufficiently large number M of periods in the structure, the $T(\lambda)$ dependence is characterised by the presence of narrow peaks [5]. The position of the maxima of $T(\lambda)$ changes with a change in the angle of incidence θ, i.e., a change in the angle makes it possible to adjust the position of the resonance for the applied radiation source. Additional opportunities for oblique incidence occur when use is made of different polarisations of the incident light. The main role of oblique incidence (as will be shown below) is to adjust the contrast of the wave vector projections k_{1x}/k_{2x} in the structure layers, which is equivalent to changing the contrast of the refractive indices of the layers at normal incidence.

V.V. Kapaev P.N. Lebedev Physical Institute, Russian Academy of Sciences, Leninsky prosp. 53, 119991 Moscow, Russia; National Research University of Electronic Technology (MIET), pl. Shokina 1, 124498 Moscow, Zelenograd, Russia;
e-mail: kapaev@sci.lebedev.ru;
M.N. Zhuravlev National Research University of Electronic Technology (MIET), pl. Shokina 1, 124498 Moscow, Zelenograd, Russia

Received 13 July 2018
Kvantovaya Elektronika **48** (10) 954–961 (2018)
Translated by I.A. Ulitkin

2. Method for calculating the field in a finite layered periodic structure

In the case of a finite layered periodic structure, Maxwell's equations are usually solved numerically using the transfer matrix method [5]. This method is simple to implement, but has insufficient numerical stability due to finite precision of calculations. The formulas for the field simultaneously have terms containing the factors $\exp(ikh)$ and $\exp(-ikh)$ (h is the layer thickness); in the presence of the imaginary part of the wave number k and a large thickness h, this method requires a very high accuracy of calculation of the coefficients at these exponents. For the real refractive indices of the layers, this instability manifests itself mainly for the parameters corresponding to the forbidden band, when the Bloch wave vector is imaginary. In the case of normal incidence, the instability of calculations appears already when the number of layers is $N \approx 100$. With oblique incidence, the effective wavelength in the medium increases (especially at large angles of incidence) and the method does not allow the dependence on the angle to be traced already for $N \approx 20$.

An alternative is the method of the scattering matrix S [11], which relates the waves incident on the structure on the right and left with those reflected to the right and left. For a layered structure, the field U_j in each jth layer with a constant refractive index n_j can be represented as

$$U_j = \exp(ik_y y)\{A_j \exp[ik_{jx}(x - x_j)] + B_j \exp[-ik_{jx}(x - x_j)]\}, \quad (1)$$

where $k_y = (2\pi/\lambda)\sin\theta$; $k_{jx} = (2\pi/\lambda)\sqrt{n_j^2 - \sin^2\theta}$ is the x-component of the wave vector in the jth layer (xy is the plane of incidence); and x_j is the coordinate of the interface between the jth and $j+1$th layers with refractive indices n_j and n_{j+1}. By U in (1) we mean the z-component of the electric field E_z for s-polarisation or of the magnetic field H_z for p-polarisation. Continuity conditions at interfaces

$$U_j = U_{j+1}, \quad \frac{1}{f_j}\frac{dU_j}{dx} = \frac{1}{f_{j+1}}\frac{dU_{j+1}}{dx} \quad (2)$$

($f_j = 1$ for s-polarisation and $f_j = n_j^2$ for p-polarisation) give the relationship of the coefficients in the adjacent jth and $j+1$th layers:

$$\begin{pmatrix} A_{j+1} \\ B_{j+1} \end{pmatrix} = D^j \begin{pmatrix} A_j \\ B_j \end{pmatrix} = \begin{pmatrix} 0.5\exp(ik_{jx}h_j)\left(1 + \frac{k_{jx}}{k_{(j+1)x}}\frac{f_{j+1}}{f_j}\right) & 0.5\exp(-ik_{jx}h_j)\left(1 - \frac{k_{jx}}{k_{(j+1)x}}\frac{f_{j+1}}{f_j}\right) \\ 0.5\exp(ik_{jx}h_j)\left(1 - \frac{k_{jx}}{k_{(j+1)x}}\frac{f_{j+1}}{f_j}\right) & 0.5\exp(-ik_{jx}h_j)\left(1 + \frac{k_{jx}}{k_{(j+1)x}}\frac{f_{j+1}}{f_j}\right) \end{pmatrix} \begin{pmatrix} A_j \\ B_j \end{pmatrix}, \quad (3)$$

where h_j is the thickness of the jth layer.

The transfer matrix method consists in the sequential calculation of (3) when j varies from 1 to N. For the left-incident wave, $A_0 = 1$, $B_0 = r$, $A_{N+1} = t$, and $B_{N+1} = 0$. As a result, we obtain the relations that allow one to determine the reflection (r) and transmission (t) coefficients of the structure:

$$\begin{pmatrix} t \\ 0 \end{pmatrix} = D\begin{pmatrix} 1 \\ r \end{pmatrix} = \prod_j D^j \begin{pmatrix} 1 \\ r \end{pmatrix}. \quad (4)$$

The total transfer matrix D is the product of the transfer matrices of the layers D^j.

In the scattering matrix method, the reflection and transmission coefficients are found from the relation

$$\begin{pmatrix} t \\ r \end{pmatrix} = S\begin{pmatrix} 1 \\ 0 \end{pmatrix}. \quad (5)$$

The scattering matrix $S \equiv S^{N+1}$ for N layers is calculated sequentially using (3) and the relationship

$$\begin{pmatrix} A_j \\ B_0 \end{pmatrix} = S^j \begin{pmatrix} A_0 \\ B_j \end{pmatrix}. \quad (6)$$

The relationship of the elements of the matrices S^{j+1} and S^j for adjacent layers has the form

$$\begin{aligned} S_{11}^{j+1} &= D_{11}^j S_{11}^j - (D_{11}^j S_{12}^j + D_{12}^j) G D_{21}^j S_{11}^j, \\ S_{12}^{j+1} &= (D_{11}^j S_{12}^j + D_{12}^j) G, \\ S_{21}^{j+1} &= S_{21}^j - S_{22}^j G D_{21}^j S_{11}^j, \\ S_{22}^{j+1} &= S_{22}^j G, \\ G &= (D_{21}^j S_{12}^j + D_{22}^j)^{-1}. \end{aligned} \quad (7)$$

The danger in numerical calculations is the terms with D_{12}^j and D_{22}^j containing factors $\exp(-ik_{jx}h_j)$ (if k has an imaginary part, it can lead to a nonphysical growth of the field with increasing x). In the transfer matrix method, the amplitudes of such waves are successively recalculated from boundary to boundary. As a result, the error accumulates, and the total transfer matrix includes terms containing products $\prod_j \exp(-ik_{jx}h_j)$. In the scattering matrix method recalculating the next layer, the terms in (7) containing D_{12}^j (first and second equations) are dangerous from the point of view of stability. However, such terms are included in (7) with a multiplier G containing D_{22}^j in the denominator. As a result, compensation occurs, and nonphysical growth of the field does not happen. Calculations by the scattering matrix method are more cumbersome than those by the transfer matrix method.

In this paper, along with the scattering matrix method, we used another, unconventional method, i.e. recurrence relation method for a plane-layered structure. In this method, the field in the jth layer is expressed as

$$U_j = A_j \exp(ik_y y)\{\exp[ik_{jx}(x - x_j)] + r_j \exp[-ik_{jx}(x - x_j)]\}. \quad (8)$$

Substituting (8) into (2) and excluding A_j, we obtain the recurrence relation for the reflection coefficients r_j:

$$r_j = \exp(2ik_{jx}h_j)\frac{r_{j(j+1)} + r_{j+1}}{1 + r_{j(j+1)}r_{j+1}}, \quad (9)$$

where

$$r_{jj+1} = \left(\frac{k_{jx}}{f_j} - \frac{k_{(j+1)x}}{f_{j+1}}\right)\left(\frac{k_{jx}}{f_j} + \frac{k_{(j+1)x}}{f_{j+1}}\right)^{-1} \tag{10}$$

is the reflection coefficient from the interface between the media with refractive indices n_j and n_{j+1}.

When radiation from the left is incident on a structure containing N layers, in a right semi-infinite ($j = N + 1$) medium, we have $r_{N+1} = 0$. With this in mind, we can successively calculate r_j in layers (9), and then using the first relation of the field continuity at interfaces (2), we can express the amplitudes A_j in the layers through amplitude A_0 of the incident wave and, therefore, find the field distribution in the structure, $U(x)$, the reflection coefficient, $r = r_0$, and the transmission coefficient, $t = A_{N+1}$, for amplitude, as well as the corresponding coefficients of R and T for intensity. The formula for r_j (9) contains only a positive exponent, which leads to a significantly greater stability of the calculation procedure as compared with the case of the standard transfer matrix. The calculation procedure is less time consuming than that by the scattering matrix method. Comparison of the results obtained by the two methods can serve as an additional method for controlling the accuracy of calculations. A similar scheme for calculating the reflection and transmission coefficients of a layered structure, based on the concept of the generalised scattering coefficient (GSC) method, is analysed in [12], where a number of examples show its greater stability compared to other methods.

As in the case of normal incidence, the reflection coefficient at oblique incidence from a finite layered periodic structure containing M periods is expressed by the expression [13], which relates the reflection coefficient and the modulus of the Bloch wave vector k for an infinite periodic structure:

$$R = \frac{|C|^2}{|C|^2 + [\sin(kd)/\sin(Mkd)]^2}, \tag{11}$$

where

$$|C|^2 = \frac{|r_1|^2}{1-|r_1|^2}; \tag{12}$$

r_1 is the reflection coefficient from a structure containing one period; and d is the period of the structure. Below, we will consider structures whose period contains two layers with refractive indices n_1 and n_2. The dispersion equation for determining k (k_s and k_p for s- and p-polarisations) has the form

$$\cos(k_{s,p}d) = \cos(k_{1x}l_1)\cos[k_{2x}(d-l_1)] - \frac{1}{2}\left(\frac{c_{s,p}k_{1x}}{k_{2x}} + \frac{k_{2x}}{c_{s,p}k_{1x}}\right)\sin(k_{1x}l_1)\sin[k_{2x}(d-l_1)], \tag{13}$$

where

$$c_s = 1, \quad c_p = (n_2/n_1)^2; \tag{14}$$

l_1 is the thickness of the layer with the refractive index n_1; and

$$k_{1x,2x} = \frac{2\pi}{\lambda}\sqrt{n_{1,2}^2 - \sin^2\theta}\,.$$

The relation similar to (11) is universal and valid both in optics and in quantum mechanics for finite structures with a periodic distribution of a potential of arbitrary form [14, 15].

It follows from (11) that for a structure containing M periods, there are $M - 1$ zero values of the reflection coefficient R (unit maximum of transmission T) in each allowed band. For bands beginning from the second one (the bands are numbered in accordance with an increase in the radiation frequency ν), an additional transmission maximum T is possible, provided that $T = 1$ [$C = 0$ in (12)] for a single element. The increase in the field amplitude at transmission maxima $T(\nu)$ is caused by the interference of counterpropagating Bloch waves. This interference is also responsible for the formation of forbidden bands, and therefore the field value at the maximum E_{max} correlates with the width of the corresponding forbidden band. In this connection, of interest is to preliminarily investigate the properties for band gap widths E_g. We are mainly interested in the conditions for obtaining the maxima of the dependences $E_g(\theta, l_1)$. Along with the maxima, there are additional features associated with the zero forbidden band width [5]. In this case, the distribution of the field in all periods is the same. It follows from (13) that two types of such features are possible. The first type corresponds to the factor $(1/2)[c_{s,p}k_{1x}/k_{2x} + k_{2x}/(c_{s,p}k_{1x})]$ equal to unity. This is possible only for p-polarisation, is achieved at an angle that is analogous to the Brewster angle:

$$\sin\theta = \frac{n_1 n_2}{\sqrt{n_1^2 + n_2^2}}, \tag{15}$$

and requires the condition

$$n_2 < \frac{n_1}{\sqrt{n_1^2 - 1}} \tag{16}$$

to be met, i.e., a fairly high contrast of the refractive indices of the layers.

The second type is realised when the factors $\sin(k_{1x}l_1)$ and $\sin[k_{2x}(d-l_1)]$ are simultaneously equal to zero, which corresponds to the condition under which an integer of half-waves fits on each of the structure layers. One can easily see that this is possible only for 'higher' bands starting from the second; this feature occurs simultaneously for s- and p-polarisations.

In the case of normal incidence, the efficiency of the interaction of Floquet counterpropagating modes depends substantially on the ratio of the refractive indices of the layers, n_1/n_2 [5]. With oblique incidence, the result is determined by the ratio of the projections of the wave vectors k_{1x} and k_{2x} in the layers, which varies depending on the angle of incidence. Thus, a change in the angle of incidence is in some way equivalent to a change in the refractive indices of the layers in the case of normal incidence. For a layer with large n, the value of k_x varies only slightly with the angle, and for a layer with n close to unity, it varies significanly. The position of the transmission resonances $T(\lambda)$ depends on the angle of incidence, which allows adjustment for the existing radiation sources.

To calculate the reflection coefficient from formula (11) and the transmission coefficient from the relation $T = 1 - R$ for each wavelength, the dispersion equation (13) should be solved numerically. From the point of view of the numerical procedure, it is easier to use the methods of the scattering matrix and recurrence relations described above, which allow R, T and the field distribution in the structure to be calculated in a single procedure.

3. High contrast of the refractive indices of the layers

Let us first consider the situation when the refractive index of one of the layers is equal to the refractive index of the medium, i.e. $n_2 = 1$. This situation in a certain sense corresponds to artificial opals, although the approximation of a one-dimensional photonic crystal for them is adequate only at small angles of incidence. We consider the model problem of a one-dimensional photonic crystal with $n_1 = 1.46$ and $n_2 = 1$ in the whole range of angles of incidence as a limiting case, which allows us to achieve a maximum change in k_{1x}/k_{2x} with a change in θ.

Instead of the radiation frequency $\nu = c/\lambda$, it is convenient to use, as in [5], the dimensionless quantity d/λ. In this case, the value of $(d/\lambda)_g$ will be used below as the band gap E_g. The functions $T(d/\lambda)$ at oblique incidence are the same as at normal incidence: there are forbidden bands (stop bands) with transmission close to zero, between which oscillating dependences $T(d/\lambda)$ with an $M-1$ unit maximum in each allowed band are observed. The character of the distributions of the electric field E for s-polarisation and of the magnetic field H for p-polarisation with parameters corresponding to unit transmission maxima is quite similar to the case of normal incidence [5]; in particular, for the first transmission maxima $T(\lambda)$ to the right and left of the forbidden bands there is a field maximum in the centre of the structure. The field value at the maximum $|E|_{max}$ can significantly exceed the amplitude of the incident field. The field maximum in the central region of the structure is localised in a layer with large and small refractive indices for the transmission maxima on the left and on the right of the forbidden bands, respectively.

Since the widths of the forbidden bands are determined by the same factors as the values of the field maxima, i.e. the interference of counterpropagating Bloch waves, it is convenient to preliminarily analyse the behaviour of the band gap E_g with changing the angles of incidence and layer thicknesses, because this problem contains fewer parameters. We first analyse the behaviour of the width of the first forbidden band. As already noted, the features associated with the zero forbidden band width due to the presence of an integer of half-waves in each of the layers are absent for the first band. Figure 1a shows the dependences of E_g on the ratio l_1/d of the thickness of the first layer l_1 to the structure period d for s- and p-polarisations at various angles of incidence θ. Noteworthy is a significant increase in E_g and a shift of the maximum of the dependence $E_g(l_1)$ towards small l_1 with increasing angle θ. Both of these features are explained by an enhancement of the contrast in the x-component of the wave vectors in media with refractive indices n_1 and n_2 with increasing θ. For $n_2 = 1$, as the angle of incidence changes, the ratio k_{1x}/k_{2x} changes from n_1 to infinity, i.e. the system implements a high contrast regime of the x-components of the wave vectors. A characteristic appearance of the dependence of E_g on the angle of incidence is presented in Fig. 1b. For s-polarisation, we observe a monotonic growth of E_g, which can increase several times. For p-polarisation, we observe a decrease in E_g at small angles up to the Brewster angle θ_B (15). When $\theta = \theta_B$, the value of E_g vanishes, after which it increases due to an enhancement of the contrast of the x-components of the wave vectors, as in the case of s-polarisation. At large angles of incidence, the first band gap width is larger for s-polarisation than for p-polarisation.

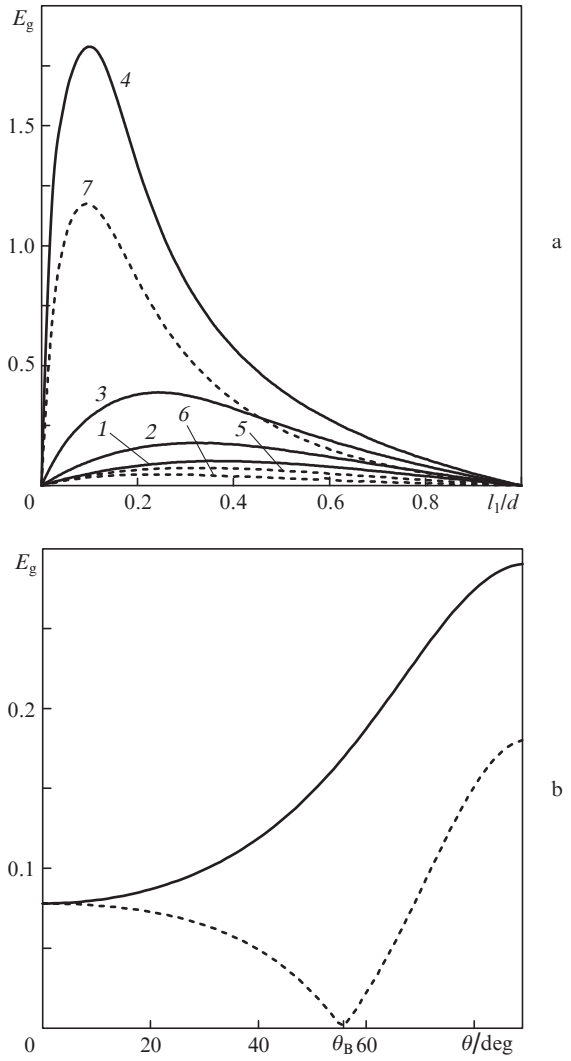

Figure 1. Dependences of the width of the first forbidden band gap E_g on (a) the layer thickness l_1 with a refractive index $n_1 = 1.46$ for angles of incidence $\theta = (1)$ 0, (2, 5) 40°, (3, 6) 60° and (4, 7) 80°, as well as (b) on the angle of incidence for $l_1 = 0.6d$. Solid curves correspond to s-polarisation, and dashed curves – to p-polarisation.

As shown in [5], the largest growth of the field in the structure occurs for the first maxima of $T(d/\lambda)$ located to the right and left of the boundary of each forbidden band; therefore, below we restrict ourselves to considering the fields only for these maxima. The dependence of the maxima of the electric field modulus $|E|_{max}$ on the angle of incidence for the transmission maxima T to the right and to the left of the first forbidden band are shown in Fig. 2 for the structure with the number of periods $M = 30$. For the left maxima, the changes in $|E|_{max}$ with θ correspond to the above dependences of the width of the first forbidden band on the angle of incidence. A decrease in $|E|_{max}$ for p-polarisation with a minimum at the Brewster angle and a significant (more than twice) increase in the field for s-polarisation are observed.

The tendency towards an increase in the field maximum with increasing angle arises from the increased interference of the counterpropagating Bloch modes, which is due to an enhancement of the contrast of the x-components of the wave numbers in the layers k_{1x}/k_{2x} and is similar to an increase in the refractive index of one of the layers in the case of normal incidence. For p-polarisation, the minimum of the depen-

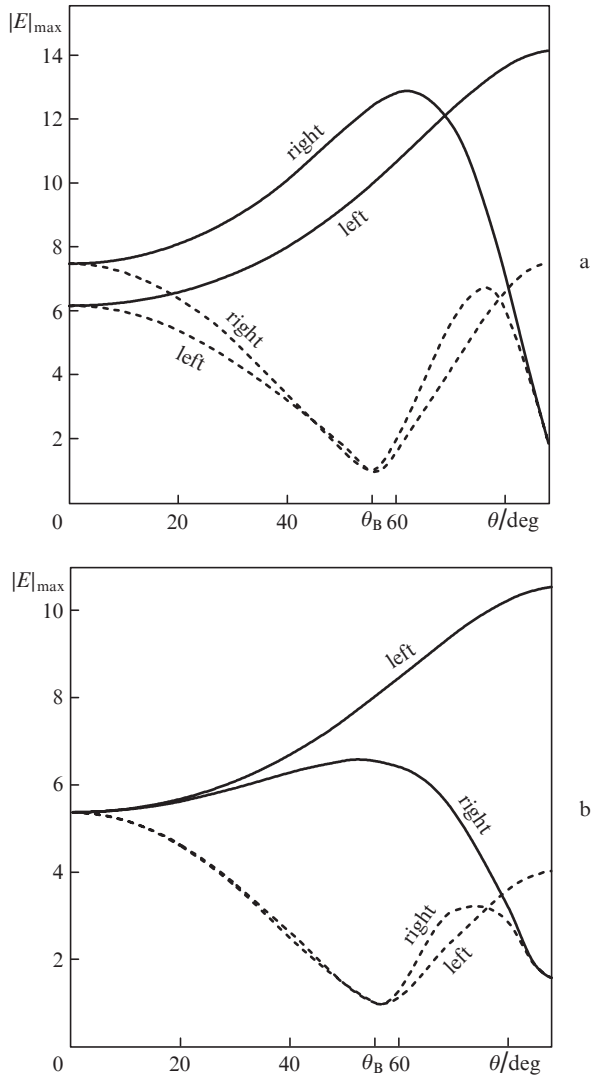

Figure 2. Dependences of the maximum electric field $|E|_{max}$ in a finite one-dimensional photonic crystal ($M = 30$) with $n_1 = 1.46$, $n_2 = 1$ at $l_1 =$ (a) $0.4d$ and (b) $0.6d$ on the angle of incidence for s-polarisation (solid curves) and p-polarization (dashed curves) with parameters corresponding to the first transmission maxima on the left and on the right of the first forbidden band.

dence $|E|_{max}(\theta)$ corresponds to the Brewster angle $\theta_B = 55.6°$ for a medium with $n_1 = 1.46$. For the maxima to the right of the forbidden band, $|E|_{max}$ decreases at large θ for both s-and p-polarisations. This is due to the fact that for the right boundary of the forbidden band, the maximum transmission of one period tends to reach the boundary of the band. In this case, the field distribution will be the same in all periods, and the field value at the maximum $|E|_{max}$ will become equal to unity. From the dispersion relation (13) at $k_{2x} \to 0$ (at $\theta \to 90°$) it follows that we have $\cos(kd) = -1$ for both polarisations at $k_{1x}l_1 = \pi$. However, the condition $k_{1x}l_1 = \pi$ corresponds to the unit transmission of one period, and $\cos(kd) = -1$ corresponds to the boundary of the first forbidden band. When $k_{1x}l_1 = \pi$, but $k_{2x} \neq 0$, we have $\cos(kd) = -\cos[k_2(d-1)] > -1$, i.e., at an angle θ other than 90°, the unit transmission maximum of a single period is located in the allowed band at any l_1. A decrease in the angle from 90° leads to an increase in the ratio d/λ, corresponding to $T = 1$ for a single period, and to a decrease in d/λ for the boundary of the forbidden band. Consequently, the maximum for a single period is shifted to the second allowed band. This explains a decrease in the field maximum on the right for both s-and p-polarisations at large angles for the right transmission maximum.

Let us now analyse the transmission maxima near the highest forbidden bands. For these bands, the forbidden band width can be equal to zero, provided that an integer p or q of half-waves fits on each of the structure layers: $k_{1x}l_1 = \pi p$, $k_{2x}(d - l_1) = \pi q$. These relations yield an equation that determines the dependence of the angle θ_c, at which the widths of bands simultaneously vanish for s- and p-polarisations, on the relative width of the layer with the refractive index n_1:

$$\frac{l_1}{d} = \left(\frac{q}{p}\frac{k_{1x}}{k_{2x}} + 1\right)^{-1}. \qquad (17)$$

The sum $p + q$ determines the number of the forbidden band, since when (17) holds, from (13) we obtain $\cos(kd) = (-1)^{p+q}$. Figure 3 [curve (*1*)] shows the dependence of the critical angle θ_c on l_1 for the second forbidden band of the structure with $n_1 = 1.46$ and $n_2 = 1$. It can be seen that there is a critical value of the thickness of the first layer, $l_1 = l_c$, above which the width of the second forbidden band does not vanish in the entire range of angles of incidence.

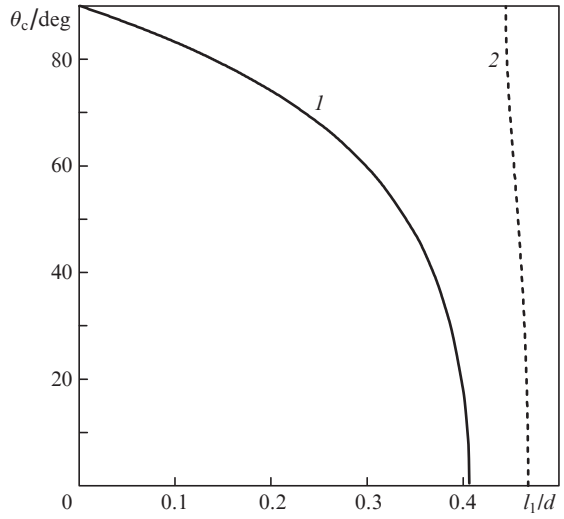

Figure 3. Dependences of the critical angle θ_c, at which the width of the second forbidden band vanishes, on the layer thickness l_1 with the refractive index n_1 at (*1*) $n_1 = 1.46$, $n_2 = 1$ and (*2*) $n_1 = 1.65$, $n_2 = 1.45$.

At $l_1 < l_c$ there is an angle of incidence at which the width of the forbidden band vanishes. In the case of low contrast of the refractive indices of the layers [curve (*2*)], the width of the second forbidden band vanishes only in a narrow range of values of l_1. Figure 4 shows an example of dispersion curves calculated by formula (13) for the case when the widths of the second forbidden bands vanish at an angle of incidence of 50° and $n_1 = 1.46$ and $n_2 = 1$. This corresponds to the ratio $l_1/d = 0.3409$. One can see from Fig. 4 that for small k the dispersion law is linear, but the slopes of the $E_g(k)$ dependence for s- and p-polarisations are different.

Figure 5 shows the dependences of the width of the second forbidden band on l_1 for different angles of incidence. A characteristic feature of these dependences is the presence of two maxima of E_g and the vanishing of E_g between them. The

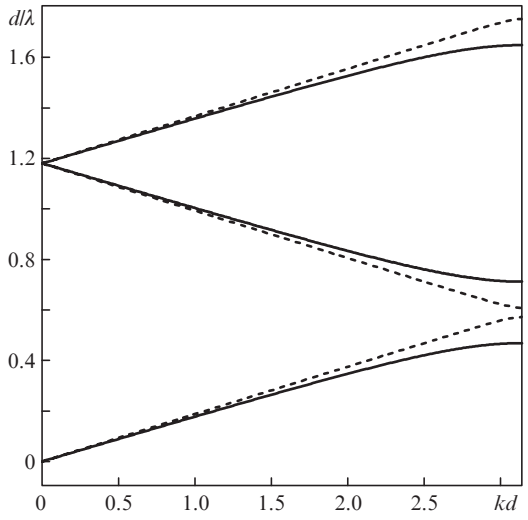

Figure 4. Dispersion law for the angle of incidence $\theta = 50°$ and $l_1/d = 0.3409$ for s-polarisation (solid curves) and p-polarisation (dashed curves).

position of zero is shifted with increasing angle in accordance with the dependence (*1*) in Fig. 3. For p-polarisation, the maximum values of the band width first decrease with increasing θ up to the Brewster angle (55.6°), then increase, and finally become comparable with the E_g values at large angles for s-polarisation. When $l_1 > l_c$, the dependences of E_g and $|E|_{max}$ on θ are quite similar to those considered above for the first forbidden band (see Figs 1b and 2). The absolute values of these quantities become comparable (even somewhat larger). When $l_1 < l_c$, the behaviour of $E_g(\theta)$ turns out to be more complicated: along with zero $E_g(\theta)$ for p-polarisation at the Brewster angle θ_B, an additional zero appears at $\theta = \theta_A$ simultaneously for s- and p-polarisations in accordance with (17). At a small l_1, the value of θ_A is greater than that of θ_B (θ_A tends to 90° at $l_1 \to 0$), and at a large l_1, the value of θ_A is less than that of θ_B (θ_A tends to zero at $l_1 \to l_c$). At $l_1 = 0.32$, the

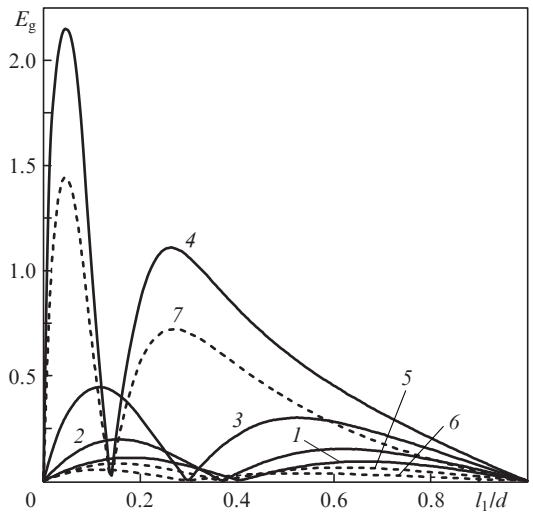

Figure 5. Dependences of the width of the second band gap E_g for s-polarisation (solid curves) and p-polarisation (dashed curves) on the first layer thickness l_1 at angles of incidence θ = (*1*) 0, (*2*, *5*) 40°, (*3*, *6*) 60° and (*4*, *7*) 80°.

values of θ_A and θ_B coincide. With an increase in the angle of incidence θ up to θ_A, the value of E_g changes only slightly, and then its rapid growth is observed with increasing θ.

The main tendencies of the change in E_g with a change in the angle of incidence θ are reflected in the dependences of the maxima of the electric field, which turn out to be significantly more complex than those described above for $l_1 > l_c$. Figure 6 presents examples of the dependences of $|E|_{max}$ on θ for $M = 30$ at $l_1 = 0.25d$ and $0.4d$. The first case corresponds to $\theta_A > \theta_B$, the second – to $\theta_A < \theta_B$. In both cases, the values of $|E|_{max}$ change little up to the angle θ_A, then there is a sharp increase, and the values for the right maxima are much larger than for the left ones. Moreover, $|E|_{max}$ is increased by almost an order of magnitude compared with the case of normal incidence. The effect is more significant for s-polarisation. In principle, the same increase $|E|_{max}$ is also possible for the first band at small l_1. For angles $\theta = \theta_A$, the field distribution is the same in all periods and the maximum value of $|E|_{max}$ is equal to unity for both s-and p-polarisations. For angles $\theta = \theta_B$, the field

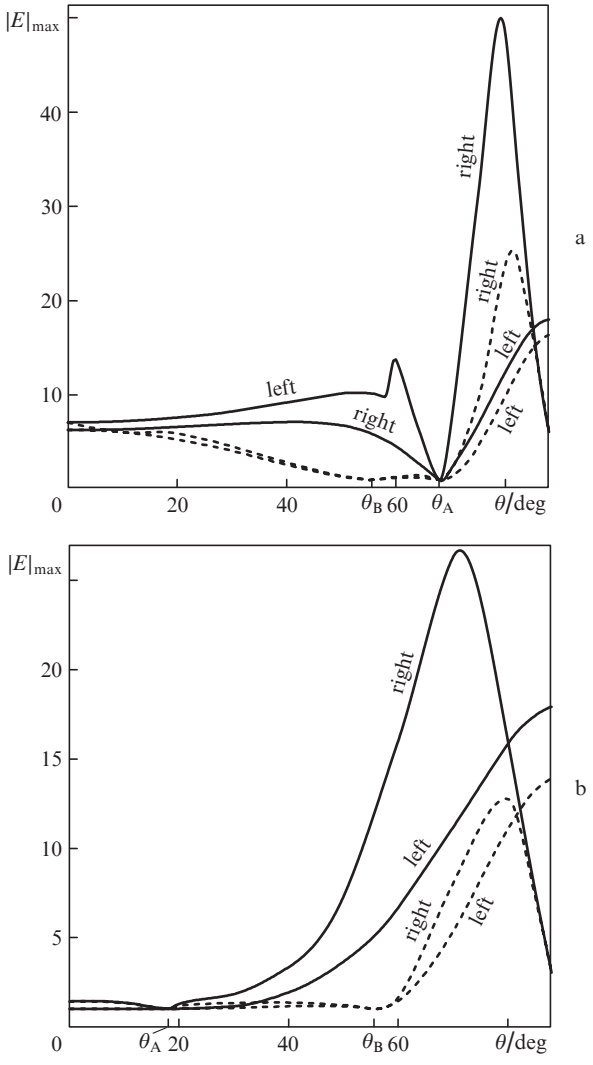

Figure 6. Dependences of the maximum field $|E|_{max}$ in the finite layered periodic structure with $M = 30$ on the angle of incidence θ for the values of d/λ corresponding to the first unit transmission maxima to the left and to the right from the second forbidden band at l_1 = (a) $0.25d$ and (b) $0.4d$. Solid curves correspond to s-polarisation, dashed curves – to p-polarisation.

$|E|_{\max} = 1$ only for p-polarisation. A decrease in $|E|_{\max}$ for left maxima at large angles for both polarisations is explained, as in the case of the maxima near the first band, by fact that the maximum $T = 1$ of the single period reaches the band boundary.

Thus, the use of oblique incidence can significantly increase the maximum field in the structure compared with the case of normal incidence. As with normal incidence, the magnitude of $|E|_{\max}$ grows linearly with increasing number of periods in the structure. The above-considered case with the parameters $n_1 = 1.46$ and $n_2 = 1$ corresponding to opal should be considered a model one, since at large angles of incidence opal is not described by a one-dimensional model. In principle, modern technologies make it possible to manufacture layered periodic structures from a wide range of materials. In order for the above features to manifest themselves, a sufficiently high contrast of the refractive indices of the layers is necessary in accordance with formula (16).

4. Low modulation of the refractive indices of the layers

The recently studied layered periodic structures based on mesoporous materials have a relatively small contrast of refractive indices. On the other hand, the number of layers in them can be quite large ($\sim$1000), which makes it possible to achieve a significant increase in field in these structures due to the interference effect of the Floquet counterpropagating modes, since the field grows linearly with increasing number of periods in the structure. In this regard, it is interesting to consider the change in field in such structures at oblique incidence of radiation. Al_2O_3-based structures typically have the refractive indices $n_1 = 1.65$ and $n_2 = 1.45$. For these refractive indices, condition (16) is not satisfied, and the band gap for p-polarisation does not vanish (the analogue of the Brewster effect is not realised). If the condition for 'an integer of half-waves on each of the layers' is fulfilled in accordance with (17), the E_g vanishes in a narrow range of l_1 values, from 0.444 to 0.468 [see curve (*2*) in Fig. 3]. Outside this range, the dependences $E_g(\theta)$ turn out to be monotonously increasing and decreasing in the case of s- and p-polarisations, respectively, for both the first and second band gaps. While for structures with a high contrast of refractive indices, a significant shift in the position of the $E_g(l_1)$ dependence maximum is observed when the angle of incidence changes (see Fig. 5), for structures in question, the shift is very small.

Thus, in this case, from the point of view of increasing the electric field, only the s-polarisation is of interest. Figure 7 shows examples of the angular dependence of the maximum field $|E|_{\max}$ in the structure for two values of l_1 and $M = 100$. In almost the entire thickness range of l_1 values, an increase in the field with increasing θ for the maxima $T(d/\lambda)$ near the first forbidden band is large compared to its increase for the maxima near the second band. An exception is the narrow region near $l_1 = 0.6d$, where at large angles an increase in the field is maximal for the left maximum at the second forbidden band (Fig. 7b). As for the first forbidden band, there prevails a situation when a larger growth of $|E|_{\max}(\theta)$ is observed for the left maximum; an opposite situation takes place in a narrow region of $l_1 \approx 0.4d$. For $M = 100$, the field can increase two-fold compared with the case of normal incidence.

In the situations presented in Fig. 7, there is no unit transmission maximum for one period (it exists only in the range of

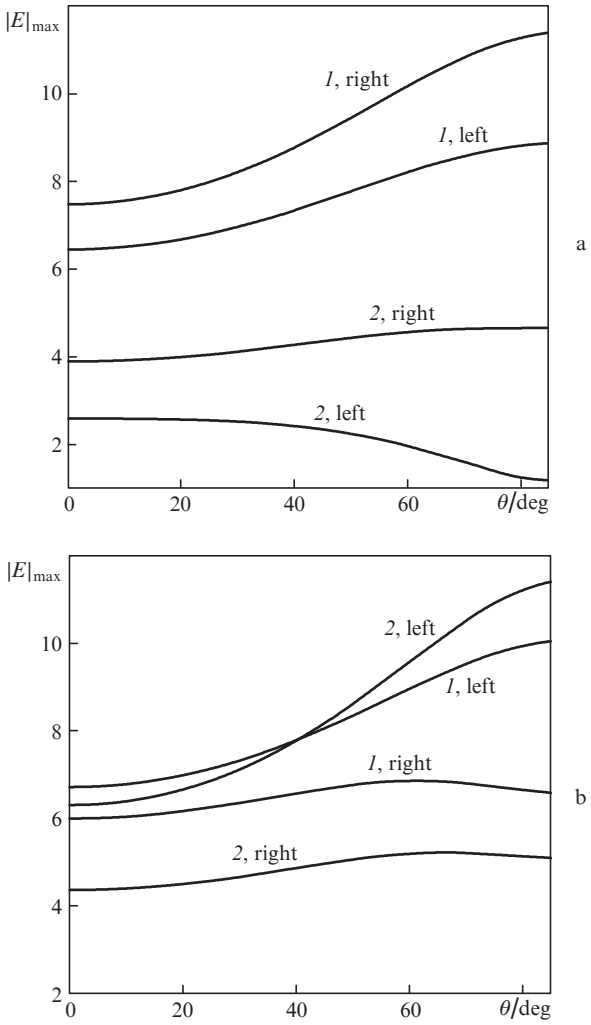

Figure 7. Angular dependences of the maximum values of the electric field $|E|_{\max}$ for the d/λ values corresponding to the first unit transmission maxima to the left and to the right of (*1*) the first and (*2*) second forbidden bands in the case of s-polarisation with $M = 100$, $n_1 = 1.65$, $n_2 = 1.45$, $l_1 =$ (a) $0.4d$ and (b) $0.6d$.

l_1 from 0.444 to 0.468); therefore, there is no explicit reduction of the field at a large angle θ for the right transmission maxima noted above for the case of high contrast of the refractive indices.

5. Conclusions

In this paper, we study the effect of increasing the electromagnetic field E in a finite layered periodic structure at oblique incidence of radiation. Specific calculations have been performed for structures whose period contains two layers with different refractive indices n_1 and n_2. The effect of the field growth is due to the interference of counterpropagating Bloch waves; therefore, the maximum increase in the field is observed under conditions corresponding to the maxima of the width of the forbidden band gap E_g. In this connection, the dependences of E_g on the parameters of the structure and the angle of incidence are preliminarily analysed. The tendency towards an increase in the field maximum with increasing angle is due to the increased interference of the counterpropagating Bloch modes caused by an enhancement of contrast of the x-components of the wave numbers k_{1x}/k_{2x} in the

layers, which is similar to an increase in the refractive index of one of the layers in the case of normal incidence.

If the refractive index of one of the layers is close to unity (or equal to it), this ratio significantly changes depending on the angle of incidence. As a result, it is possible to obtain a substantial (several times) increase in the width of the forbidden band and the maximum of the field $|E|_{\max}$ when changing the angle of incidence. Along with the maxima of E_g, there are particular situations when the width of the forbidden band vanishes at a certain angle of incidence. There are two types of such features. The first type is observed only with p-polarised radiation for structures with a sufficiently high contrast of the refractive indices (16) and serves as an analogue of the Brewster effect. The second type corresponds to the condition $k_{jx}l_j = q_j\pi$, in which an integer of half-waves fits on each of the layers, and is realised simultaneously for s- and p-polarisations in a limited range of layer thickness ratios only for the second and higher forbidden bands. The field $|E|_{\max}$ at the finite angle of incidence increases for both polarisations, but in general, the effect is greater for s-polarisation.

For structures with a low contrast of refractive indices, as is the case in mesoporous structures, the conditions for the Brewster angle are not met, and the condition of an integer of half-waves in each of the layers can be achieved only in a narrow range of l_1/d values. The effect of an increase in the field with increasing angle of incidence is observed only for s-polarisation, and at $M = 100$, the field can increase two-fold.

An additional advantage of oblique incidence of radiation is the possibility of the wavelength adjustment of the positions of the transmission resonances, for which an increase in $|E|_{\max}$ is observed.

Acknowledgements. This work was partially supported by the Ministry of Education and Science of the Russian Federation (Task No. 16.2250.2017/PCh).

References

1. Kapaev V.V. *Sov. J. Quantum Electron*., **19**, 1460 (1989) [*Kvantovaya Elektron*., **16**, 2271 (1989)].
2. Bendickson J.M., Dowling J.P. *Phys. Rev. E*, **53**, 4107 (1996).
3. Scalora M., Bloemer M.J., Manka A.S., Dowling J.P., Bowden C.M., Viswanathan R., Haus J.W. *Phys. Rev. A*, **56**, 3166 (1997).
4. Hopman W.C.L., Hoekstra H.J.W.M., Dekker R., Zhuang L., de Ridder R.M. *Opt. Express*, **15**, 1853 (2007).
5. Gorelik V.S., Kapaev V.V. *JETP*, **123**, 373 (2016) [*Zh. Eksp. Teor. Fiz*., **150**, 435 (2016)].
6. Astratov V.N., Bogomolov V.N., Kaplyanskii A.A., Prokofiev A.V., Samoilovich L.A., Samoilovich S.M., Vlasov Yu.A. *Il Nuovo Cimento D*, **17**, 1349 (1995).
7. Bogomolov V.N., Gaponenko S.V., Kapitonov A.M., Prokofiev A.V., Ponyavina A.N., Silvanovich N.I., Samoilovich S.M. *Appl. Phys. A*, **63**, 613 (1996).
8. Gorelik V.S., Lepnev L.S., Litvinova A.O. *Neorg. Mater*., **50**, 1086 (2014).
9. Liu Yisen, Chang Yi, Ling Zhiyuan, Hu Xing, Li Yi. *Electrochem. Commun*., **13**, 1336 (2011).
10. Svyakhovskiy S.E., Maydykovsky A.I., Murzina T.V. *J. Appl. Phys*., **112**, 013106 (2012).
11. Ko D., Yuk K., Inkson J.C. *Phys. Rev. B*, **38**, 9945 (1988).
12. Liu Y., Li C., Wang H., Zhou Y. *Am. J. Phys*., **85**, 146 (2017).
13. Yeh P., Yariv A., Hong C. *J. Opt. Soc. Am*., **67**, 423 (1977).
14. Vezzetti D.J., Cahay M.M. *J. Phys. D: Appl. Phys*., **19**, L53 (1986).
15. Sprung D.W.L., Wu H. *Am. J. Phys*., **61**, 1118 (1993).